Cement and Concrete Research 42 (2012) 61–73

Contents lists available at ScienceDirect

Cement and Concrete Research

journal homepage: http://ees.elsevier.com/CEMCON/default.asp

Basic creep behavior of concretes investigation of the physical mechanisms by using acoustic emission

Pierre Rossi *, Jean-Louis Tailhan, Fabrice Le Maou, Laurent Gaillet, Eric Martin

Institut Français des Sciences et des Technologies des transports, de l'Aménagement et des Réseaux (IFSTTAR, previously LCPC), Université Paris-Est, France

ARTICLE INFO

Article history:
Received 22 October 2010
Accepted 26 July 2011

Keywords:
Concrete (F)
Basic creeps
Experimental tests
Acoustic emission
Physical mechanisms

ABSTRACT

The Laboratoire Central des Ponts et Chaussées has launched a research project to study the physical mechanisms related to the basic creep of concrete to develop a numerical modeling physically based. In this context, a very important experimental work has been done to investigate, for the same concrete, different aspects of this basic creep behavior.

These experimental studies allow proposing an assumption concerning the physical mechanisms at the origin of the basic creep of concrete. This assumption is that the creation of microcracks during creep step (constant load level imposed during the creep test) generates water transfers which induce some additional self-drying shrinkage.

In other words, it is proposed that the basic creep of the concrete is mainly an additional self-drying shrinkage under stress.

1. Introduction

Creep behavior of concretes is an important phenomenon to be taken into account for evaluating and analyzing the behavior of most concrete structures.

IFSTTAR has launched a research project to study the physical mechanisms related to the basic creep of concrete to develop a numerical modeling (finite element approach) physically based.

A very important campaign of experimental studies has been performed to reach this objective. This campaign includes:

- a study on the basic creep in compression versus the basic creep in tension,
- a study on the volume effect related to the basic creep in compression,
- a study on the use of acoustic emission during a basic creep test in compression.

This paper presents a comprehensive analysis of the results obtained during these three experimental studies, analysis leading to a proposal concerning the physical origins of the basic creep of concrete.

2. Acoustic emission technique used during a compressive creep test

It is well-known that the presence of free water in concrete porosity is at the origin of the creep behavior of concretes [1].

On the other hand, there is currently no consensus on the physical mechanisms in which this free water is involved.

An assumption, which was proposed some years ago, concerns a strong coupling between the cracking process and the water transfers through concrete porosity [2].

To verify this assumption, acoustic emissions were recorded during basic creep tests in compression performed on two specimens loaded at 30% of their respective compressive strength. Each specimen corresponded to two different concretes having different compressive strengths and Young moduli. The duration of these tests was 7 days.

The main conclusion drawn from this previous study was that the basic creep strain is linearly dependent of the total number of microcracks created in the material. From this previous study, an important question has still to be solved: is the proportionality between the total number of created microcracks and the basic creep strain always valid for a much longer duration of creep load, and for different levels of creep load?

To answer this question, acoustic emissions have been recorded again during a basic creep test in compression. The main differences from the previous study [2] are the following:

- the applied creep load has lasted more than 120 days,
- 5 loading levels have been applied during the test, the smallest one being equal to 50% of the concrete compressive strength.

* Corresponding author: Tel.: +33 1 40 43 52 95; fax: +33 1 40 43 54 93.
E-mail address: pierre.rossi@lcpc.fr (P. Rossi).

0008-8846/$ – see front matter
doi:10.1016/j.cemconres.2011.07.011

Table 1
Mix design of the studied concrete.

Components	kg/m^3
Cement: CEMI 52.5 N PMES CA2	340
Dried sand-lime agregate 0/4	739.45
Dried sand-lime agregate 6.3/20	1072.14
Added water	184.22

Table 3
Loading procedure adopted during the creep test.

Loading level (%)	Loading time (days)
54	87
59	31
73	7
75	0.07
80	0.06

2.1. Concrete studied

The mix design of the studied concrete is given in Table 1. In Table 2, some mechanical characteristics of the concrete are given at the age of 28 days. The creep load was applied on the concrete at the age of 266 days.

2.2. The creep tests

The creep tests were performed on loading frames designed at LCPC. The technology of the LCPC creep frame and the test procedure has already been published in detail [3–6] and therefore will not be presented in this article.

The tested specimens are cylinders, 160 mm in diameter and 1000 mm high, and protected from drying throughout the test (the condition for a basic creep test) by a double layer of self-adhesive aluminum-paper sheet glued to the specimen (method developed by the LCPC [7]). Concurrently, autogenous shrinkage tests are performed on specimens identical to those for the creep test (and also protected from drying in the same way). The basic creep strain is therefore classically determined by subtracting from the total strain, the instantaneous elastic strain due to the loading of the specimen and the strain due to the autogenous shrinkage.

During the creep test, 5 loading levels were applied during different loading times. A loading level corresponds to a percentage of the average compressive strength of the concrete.

The 5 loading levels and the corresponding loading times are given in Table 3.

2.3. Acoustic emission

The acoustic signal is measured using 4 sensors distributed along the specimen as shown in Fig. 1. As soon as a signal is received by one or more sensors, it is amplified and filtered. If its peak amplitude exceeds 250 mV, the time at which the signal was received, the number of sensors that received the signal first, and the spectrum of the received signal are recorded. Signals that reach first one of the two end sensors are immediately eliminated to avoid recording noise from the loading frame or the helmet/specimen interface.

The processing of the data is done in the next procedure: after the record of a signal (time of emission, number of sensors that recorded it first, peak amplitude), an energy distribution in three frequency bands is produced in accordance with the following principle: for each frequency interval, the area of the curve between the lowest frequency and the highest frequency is calculated and its ratio to the total area is determined. This yields to the percentages of the energy in the low, medium and high frequency bands, which may serve to distinguish signals of different types and therefore of different physical origins. The three chosen frequency intervals are:

Interval 1, low frequencies (LF), 0–125 kHz
Interval 2, medium frequencies (MF), 125–250 kHz,
Interval 3, high frequencies (HF), 250–375 kHz.

The methodology used to compare the acoustic signatures is based on the frequency distribution of the signal. For each signal, the ratios LF/MF, LF/HF, and MF/HF (LF, MF and HF were already defined) are examined and the signal is classified according to whether these ratios belong to the intervals [0, 1/5[, [1/5 1/2[, and [1/2, 1].

2.4. Results

Results are presented in Figs. 2–9:

- The total strain versus time (Fig. 2)
- The total number of acoustic events versus basic creep strain (Fig. 3).
- The total number of acoustic events versus basic creep strain related to each loading level (Figs. 4–8)
- The increase with time of the total number of acoustic events related to the LF/MF ratio (Fig. 9).

The acoustic events number related respectively to the LF/HF and MF/HF have been very low.

Table 2
Mechanical characteristic of the concrete.

f_c (MPa)	46
f_t (MPa)	2.4
E (GPa)	46

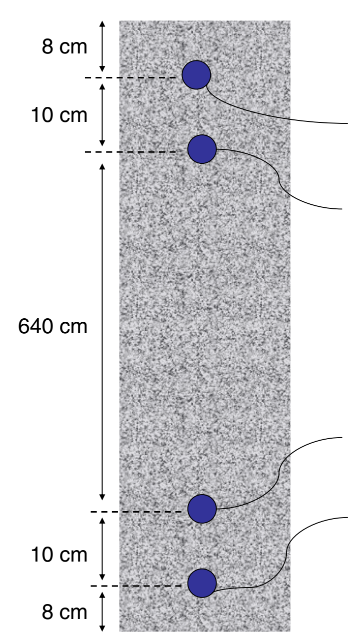

Fig. 1. Arrangement of acoustic emission sensors on the specimen (dimensions of the cylindrical specimen, h = 100 cm, ∅ = 16 cm).

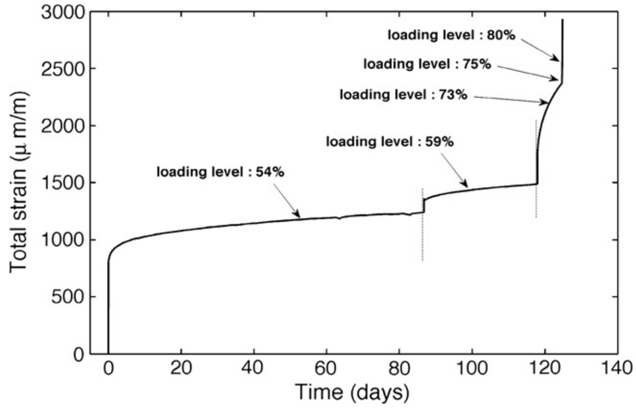

Fig. 2. Total strain versus time.

2.5. Analysis of results

Figs. 4–8 lead to the following conclusions:

- for each loading level, the basic creep strain seems globally linearly dependent on the total number of acoustic events;
- the higher the loading level, the higher the slope related to the linear relation linking the basic creep strain and the total number of acoustic events.

Table 4 presents the value of the proportionality slope, *a*, as a function of the loading level.

Fig. 9 indicates that the frequency distributions of the acoustic signal remain the same throughout the creep test, including the phases of loading.

The assumption is that the acoustic events recorded during the loading phase of the specimens are mainly due to the creation of microcracks, which is a reasonable assumption given the current knowledge.

As a matter of fact, in previous experimental works [8,9] related to the study of cracking process of concrete in mode I (microcrack and macrocrack openings in mode I), it was found that, with exactly the same acoustic emission equipment and the same chosen pass-filters, the frequency distribution of the acoustic signals was the same as in the present study.

Moreover, it is important to mention that, in a recent experimental study related to the basic creep behavior of a concrete loaded in tension [10], it has been found that it a linear relation exists between the basic creep strain in tension and the number of acoustic events recorded.

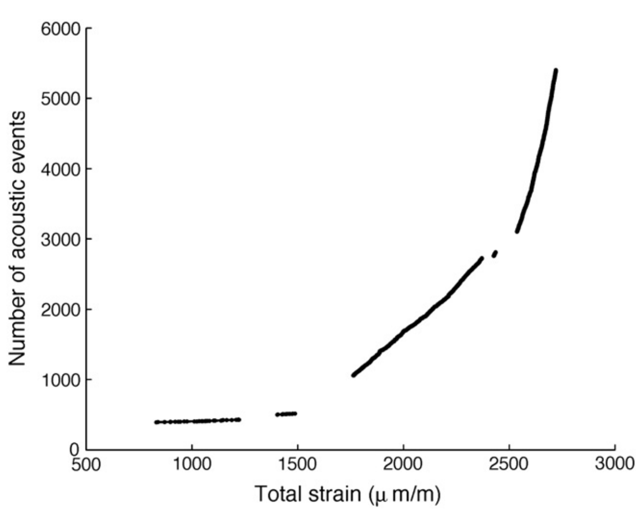

Fig. 3. Total number of acoustic events versus total strain for all the duration of the creep test.

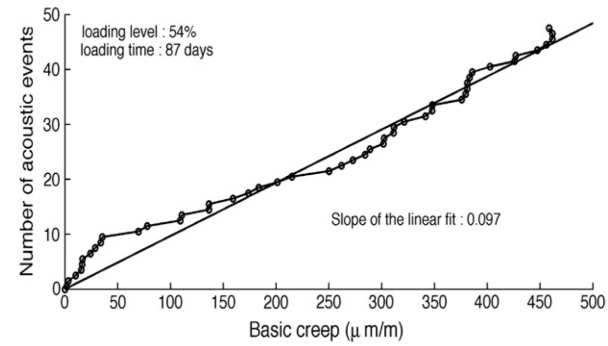

Fig. 4. Number of acoustic events versus basic creep for the 54% level of loading.

So, it can be said, without any ambiguity, that the acoustic events recorded during the basic creep test are related to the creation of microcracks and that, in consequence, the basic creep strain is proportional to the total number of microcracks in the specimen.

Finally, the principal conclusions are the following:

1. The basic creep strain is linearly dependent on the total number of microcracks created in the material.
2. The higher the loading level, the higher the density of microcracks created, and the higher the *density of microcracks created/basic creep strain* ratio.

3. Basic creep in tension versus basic creep in compression

3.1. Experimental procedures

3.1.1. Creep in compression

The creep test in compression is the one described previously.

3.1.2. Creep in tension

The LCPC creep test in tension has been designed and developed in 2008 for an industrial research contract conducted for the Institut (French) de Radioprotection et de Sureté Nucléaire (IRSN). This contract involved the study of endogenous tensile creep of a concrete nuclear power plant. The duration of the test did not exceed 3 days in that study, [10]. The design of the loading frame in tension contains a lever arm (Figs. 10 and 11). To reduce the maximum load to handle, maintain good sensitivity, and limit the size of the frame, a ratio 5/1 was adopted for the lever arms. The tested specimen is cylindrical. It has a diameter of 13 cm and a length of 50 cm.

As for the specimens related to creep test in compression, the specimens related to creep test in tension are protected from drying

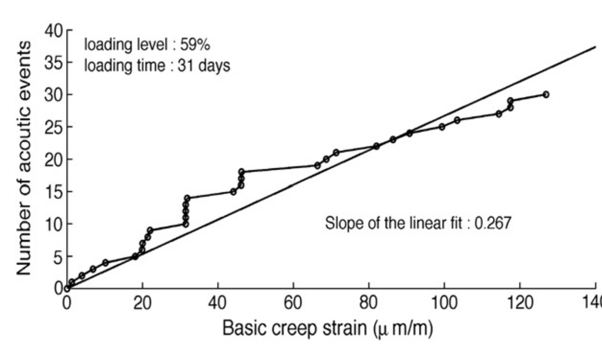

Fig. 5. Number of acoustic events versus basic creep for the 59% level of loading.

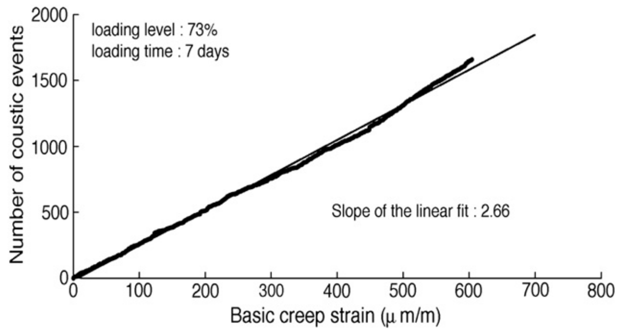

Fig. 6. Number of acoustic events versus basic creep for the 73% level of loading.

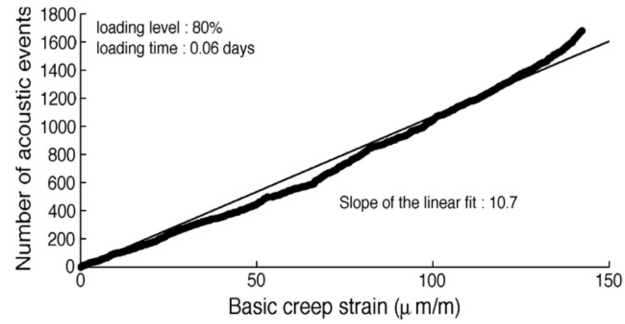

Fig. 8. Number of acoustic events versus basic creep for the 80% level of loading.

throughout the test by a double layer of self-adhesive aluminum foil bonded on the specimen. The specimen is connected to the loading frame by bonding and bolting. The specimen is glued to aluminum helmets that are connected to the loading frame by bolting (Figs. 10 and 11). A bonding system for helmets has been designed to ensure proper alignment of the tensile axes of the specimen (Fig. 12).

With the 5/1 ratio chosen for the lever arm, it requires 1,300 kg of mass to apply a maximum force of 65 kN. In order to obtain a loading sensitivity threshold of 1%, 100 disks of 13 kg each are chosen to lead to the maximum force (Figs. 10 and 11).

A delicate aspect of the device concerns the connecting points of the arm. Indeed, to obtain a proper test, it is essential to minimize the friction forces. The solution chosen for these connecting points are bull socket joints (Fig. 13).

Three displacement transducers are fixed at 120° on the central part of the specimen (Figs. 14 and 15). The measurement basis is 30 cm.

As for the study relative to basic creep in compression, simultaneously to the basic creep tests in tension, autogenous shrinkage tests on specimens identical to those used for creep are made.

The creep strain is, the same as for the creep in compression, conventionally determined by subtracting from the total strain, the instantaneous elastic strain due to the loading and the strain due to the autogenous shrinkage.

Note that, for the two configurations (tensile and compressive tests), the loading is quasi-instantaneous (it takes less than 1 s to load the specimen). So, there is no significant creep during the compressive and tensile loadings.

3.2. Experiment program

3.2.1. Concrete studied

The concrete is the same as the one described previously and detailed in Tables 1 and 2.

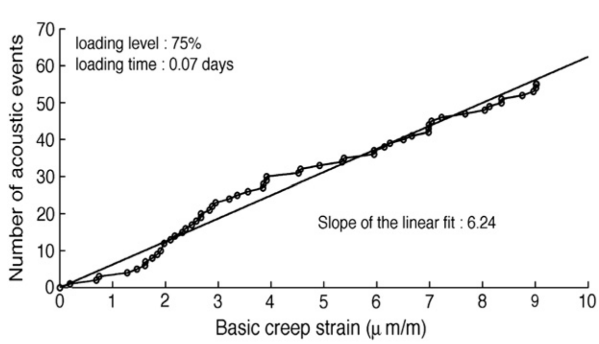

Fig. 7. Number of acoustic events versus basic creep for the 75% level of loading.

3.2.2. Test program

The creep tests in compression and in tension have been performed at concrete age of 64 days.For each type of test, one specimen was tested.

For both types of test, the load level was respectively 50% of the tensile strength and of compressive strength of the concrete at 28 days.

The test duration was 6 months for the creep test in compression and 1 month for the creep test in tension.

3.3. Experiment results

The experiment results are summarized in Fig. 16 which shows the compliance curves (strain versus time per unit of applied stress) for the two creep tests in compression and the creep test in tension.

The experimental curves related to the autogenous shrinkage of the two types of specimen (one linked to the compressive creep test, the other to the tension creep test) are presented in Fig. 17.

3.4. Analysis of results

Fig. 17 shows a very small autogenous shrinkage of the concrete given by the two types of specimen. Some variations are due to sensitivity to variations of temperature existing in the test room during the creep tests. This result is not astonishing when we consider the age of the concrete (64 days) at the loading time.

Fig. 16 shows that compliance in compression is significantly higher than compliance in tension. We can consider that the ratio, R, between these two compliances is close to 3 (for the same test duration of 1 month). We can also perform a more detailed evaluation of the evolution of this ratio R over time (taking into account an average compliance curve for the two creep tests in compression).

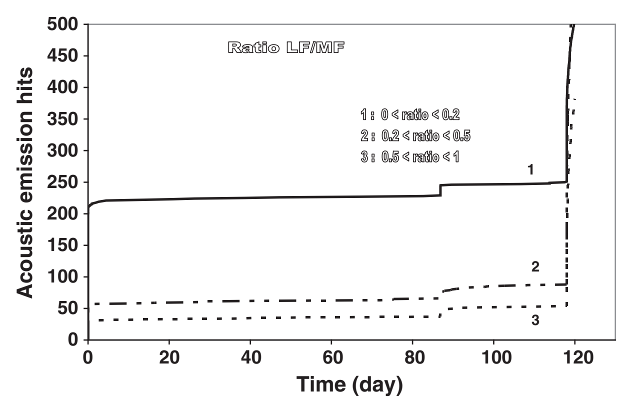

Fig. 9. Increase with time of the total number of acoustic events related to the LF/MF ratio.

Table 4
Value of *a* in function of the loading level.

Loading level (%)	54	59	73	75	80
a	0.097	0.267	2.66	6.24	10.7

Table 5 shows the evolution of this ratio for 8 different test durations: 1, 2, 3, 4, 5, 10, 20, 30 days.

One can note that the ratio, R, appears to decrease significantly over time. This would reflect the fact that the kinetics of creep in tension along time is greater than that in compression.

To confirm that concrete basic creep is significantly higher in compression than in tension, other basic creep tests in tension and in compression, carried out on the same concrete are summarized in Figs. 18–20. It is important to note that the age of concrete (A), and the loading level (L), were different for each test. These figures confirm that basic creep in compression is significantly higher than in tension for the concrete studied and the different ages of the material considered.

4. Volume effects related to the basic creep of concrete in compression

4.1. Test performed and experimental procedures implemented

4.1.1. The studied concrete

The concrete is the one just described above (Tables 1 and 2).

4.1.2. The creep tests

The creep tests were performed on two creep devices designed at LCPC.

The first device was presented previously (Section 2).Three sizes of cylinders have been tested on this device: a specimen of with diameter 160 mm and height 1000 mm (V_1), a specimen of diameter 130 mm and height 50 mm (V_2) and a specimen of diameter 160 mm and height 320 mm (V_3).

The second creep device has been designed, in the past, to test smaller specimens. But, except for this difference in dimensions, the second device is identical to the first one.

Only one size of specimen has been tested on this device: a specimen of diameter 110 mm and height 160 mm (V_4).

The respective volumes related to the 4 dimensions of specimens are given in Table 6.

Fig. 11. Photo of entire tensile creep machine.

There is a ratio of about 3 between the volume V_1 and volumes V_2 and V_3; V_2 and V_3 having similar values.

Regarding V_2 and V_3, the proximity of their respective volume was chosen to study the impact of the geometric length of the specimen on the volume effect, if any.

For the 3 types of specimen geometries, displacement (hence strain) were measured at the center of the specimen (an average of 3 values given by 3 LVDT placed at 120° on the specimens is calculated). Concerning the specimen V_1, displacements are measured on a base of 500 mm, while concerning the specimens V_2, V_3, and V_4, they are measured on bases of 400 mm, 120 mm, and 100 mm respectively.

So the measurements of the respective volumes concerned by the displacements are given in Table 6. It is noted that the difference between the volumes of material concerned by the creep strain measurement follows an arithmetic progression of about 2.

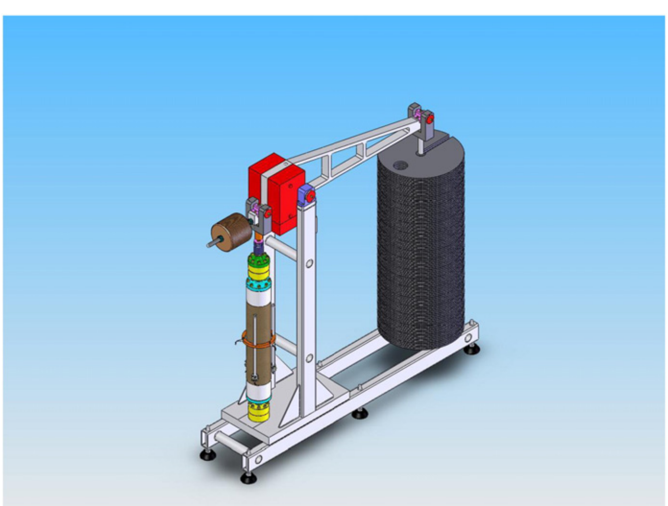

Fig. 10. Schematic overview of the tensile creep machine.

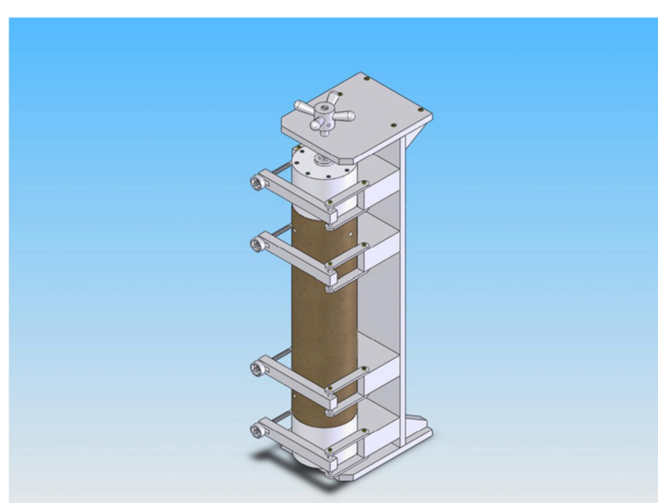

Fig. 12. Bonding system of the aluminum helmets.

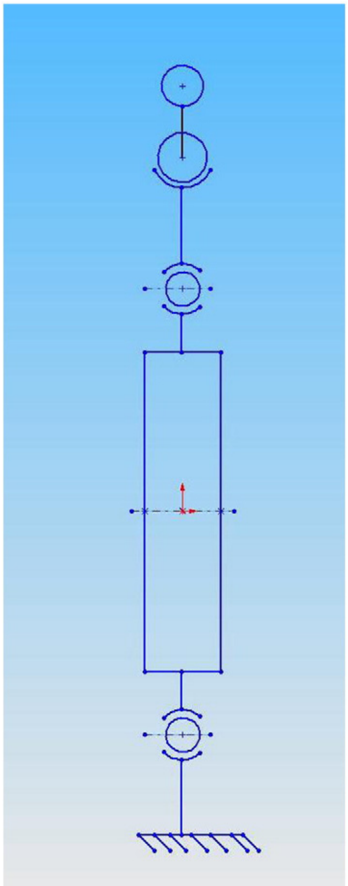

Fig. 13. Kinematic schema.

All specimens are protected from drying throughout the test by a double thickness of self-adhesive aluminum foil bonded on specimens.

All specimens are ground and polished before being placed on the creep frame.

In parallel and simultaneously to the creep tests, autogenous shrinkage tests are carried out on specimens identical to those used for creep (and again, the same technique to protect from drying is used).

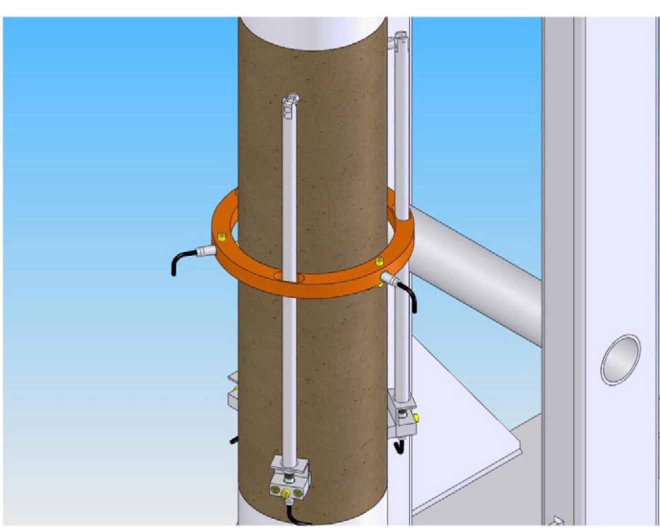

Fig. 14. Schema of the longitudinal measurement system.

Fig. 15. Photo of the longitudinal displacement system.

The creep strain is conventionally determined by subtracting from the total strain, the instantaneous elastic strain due to the specimen loading and the strain due to autogenous shrinkage.

The main difference between the 4 specimens concerns the manner of placing them inside the machine. Indeed, the first creep machine was originally designed for tests on V_1 specimens. Therefore, it was decided to place the V_2 specimen between two other cylinders of the same concrete to obtain a total height of 1000 mm. Only the 500 mm long specimen is instrumented.

Regarding V_3 specimens, 3 cylinders are placed inside the device, and are instrumented.

Regarding V_4 specimens, 2 cylinders are placed inside the device and are also instrumented.

Figs. 21–24 show the 4 experimental setups.

In summary, the tests are conducted on 1 specimen of type $V_{1,}$ 1 specimen of type $V_{2,}$ 3 specimens of type $V_{3,}$ and 2 specimens of type V_4.

All creep tests are performed at the same concrete age of 64 days.

Finally, all specimens are loaded at a stress level equal to 50% of the concrete compressive strength (determined at a concrete age of 28 days).

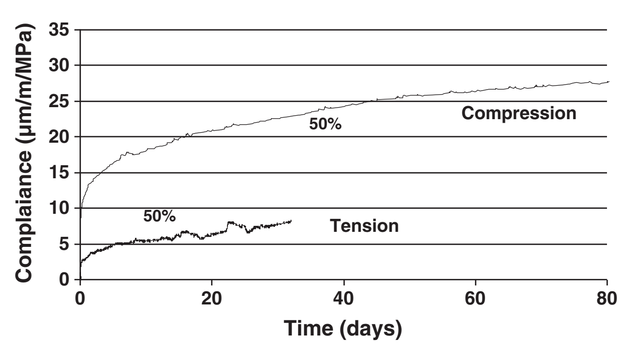

Fig. 16. Compliance curves related to the basic creep in compression and in tension (same loading level and same concrete age).

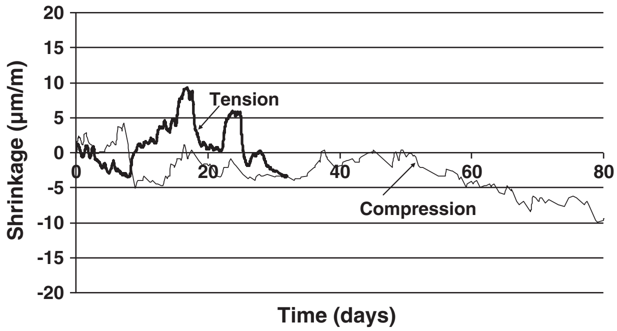

Fig. 17. Shrinkage curves related to the two types of specimen and two types of creep test.

4.2. Experiment results

In Fig. 25 are presented the curves of compliance (creep strain per unit of stress) versus time for all tested specimens.

Fig. 25 shows that the 4 types of specimens tested lead to similar compliance curves, if usual scattering related to this compliance in compression is considered [11]. In others words, it is acceptable to say that there is no significant volume effects related to creep in compression.

This result is very different from what was found during the study performed by Omar et al. [19] on the volume effects related to the flexural creep.

Indeed, in this project, 3 dimensions of prismatic specimens were studied. The heights of these specimens were respectively 100, 200, and 400 mm, presenting therefore a geometric progression of about 2.

It has been shown that the flexural creep increased with the size of the specimen. This increase followed an arithmetic progression of about 50%.

5. Experiment evidences resulting from LCPC studies and from literature

5.1. Experiment evidences resulting from LCPC studies

The experiment evidences resulting from the LCPC studies above presented are the following:

1. The basic creep of concrete in tension is much lower than the basic creep in compression (for the concrete mix and concrete ages studied).
2. In compression, for the same concrete loaded at the same age and at the same loading level, volume effect does not exist.
3. The basic creep strain is linearly dependent on total number of microcracks created in the material.
4. The higher the loading level, the higher the density of microcracks created, and the higher the *density of microcracks created*/*basic creep strain* ratio.

Remark. In other research projects [13,14], different conclusions than in the present work were drawn concerning the relation between the basic creep in compression and the basic creep in tension.

That apparent contradiction can be analyzed as follows:

– Firstly, there are few results in the literature related to the comparison between the basic creep in compression and in tension of the same concrete. So, it would be wrong to say that a consensus exists concerning this comparison.
– Secondly, the comparison concerns basic creeps and not the drying ones. That means that it should be possible to observe the contrary if drying creeps were concerned (due to the important cracking at the surface of a specimen during drying creep in tension). It is acceptable to say that, in the past, the sealing procedure was inadequate and that the results obtained may not be reflective of the real basic creep situations.
– Thirdly, performing a good creep test in tension is very difficult. As a matter of fact, during this type of test, the measured displacements on the specimens are very low and very sensitive to the temperature response of the displacement transducer. This problem was not clearly discussed in the previous papers. It may be the reason why the results presented in these papers were confusing.

Table 5
Evolution of ratio R, compressive compliance/tensile compliance, during time.

Test duration (days)	1	2	3	4	5	10	20	30
R	3.45	3.34	3.27	3.22	3.19	3.08	2.98	2.92

5.2. Experiment evidences from literature

The experiment evidences from literature are the following:

1. In bending (3 points bending tests on notched prismatic specimen), for the same concrete loaded at the same age, the amplitude and the kinetics of creep increase with dimensions of the stressed specimen (the notch length/specimen height ratio was kept constant). This scale effect increases with the loading level [12].
2. Still in bending creep situation (3 points bending test on notched prismatic specimen), the rate of evolution of the microcracked zone at the macrocrack tip increases with specimen dimensions [12].

This last result can be analyzed in another way. Indeed, in a bending creep test on notched sample, the material d of the notch is, at the notch tip, strongly stressed in tension (the tensile stress/tensile strength ratio is very high), whereas the compressive zone of specimen undergoes very weak creep stresses in compression (compressive stress/compressive strength ratio is very weak). Consequently, it is justified to say that there exists a very strong scale effect relating to creep in tension for the concretes.

6. Analyses of the experiment evidences

The experiment evidence mentioned previously lead to the following conclusions:

1. The fact that scale effects exist in tension and not in compression, when the basic creep of the concrete is considered, cannot be caused by viscous purposes at the level of the hydrates (viscous effects related to the water movements on this scale which would be the driving force of creep). Indeed, there is scale effect relative to the mechanical behavior of a heterogeneous material, it is necessary that the physical mechanisms at the origin of the considered mechanical behavior occur at a scale of heterogeneity compatible with the mechanical behavior considered. However, in concrete, the literature shows that only the cracking in tension before localization generates significant scale effects [15,16]. This comment is confirmed besides by the fact that, in the study performed by Omar et al. [12], the basic creep rate is correlated to the rate of evolution of the microcracked zone at end of the notch, which increases with the size of the bending specimen.
This difference between tension and compression concerning the volume effects is easily explained through the well-known Weibull theory [17] related to the breaking of brittle materials (theory of the weakest link).
The implementation of this theory shows that, the more the density of microcracks (related to the material heterogeneity and the

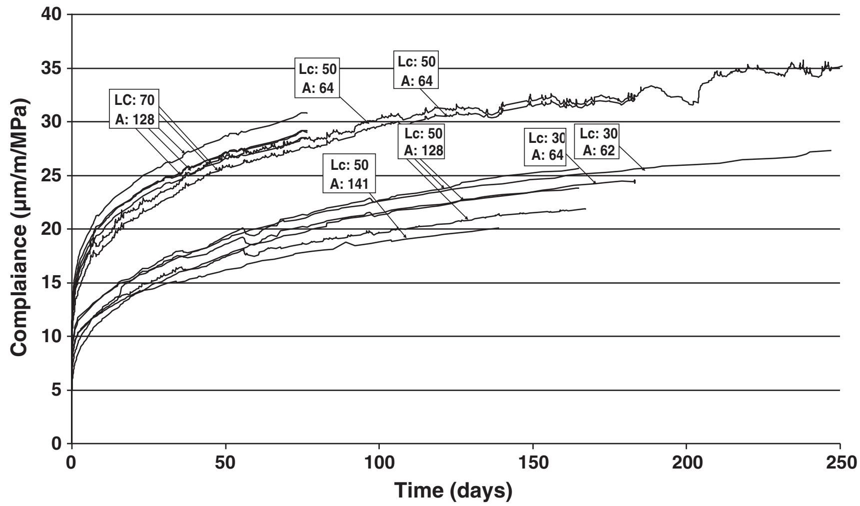

Fig. 18. Compliance curves related to the basic creep in compression for different loading level (L_C) and different concrete ages (A).

existence of weak points) before localization of cracking (synonymous with fracture of material) is important, the less are the scale effects (the weak link has less importance on the fracture of the considered volume of material). However, the density of microcracks created in a volume of concrete in tension is lower than that created within the same volume in compression. This difference is related to the fact that the cracking in compression is more stable than that in tension (in compression, the local tensile stresses are generated through the heterogeneous Poisson's ratio of the concrete).

2. The fact that the *microcracks creation* versus *creep strain* curve depends on the initial state of microcracking (created before the creep step) cannot either be explained by viscous mechanisms at the level of the hydrates. Indeed, if these viscous mechanisms were the driving forces of basic creep, an increment of creep strain should create an increment of density of microcracks independently of the initial density of microcracks.
3. The fact that basic creep in tension is lower than that in compression cannot be explained by the existence of viscous mechanisms at the level of the hydrates.

Consequently, it is relevant to say that the concrete microcracking and its evolution during time constitutes the principal driving force of the basic creep.

7. Proposal of a physical mechanism at the origin of the basic creep of concrete

When a static loading is applied to a concrete specimen, it will crack. The density of microcracks created depends on the level of the static loading. The end of the static loading corresponds to time t_0 of the creep test.

The microcracks generate a brutal hygral imbalance within the concrete. Indeed, the vacuums (which are the cracks at the moment of their creation) generate local hygral shocks which result in the appearance of gradients of concentration in water molecules as well as gradients of pressure.

Thus, the existence of these two types of gradient will induce water vapor movements (Fick's law) as well as liquid water movements (Darcy's law) from the capillaries surrounding the microcracks towards

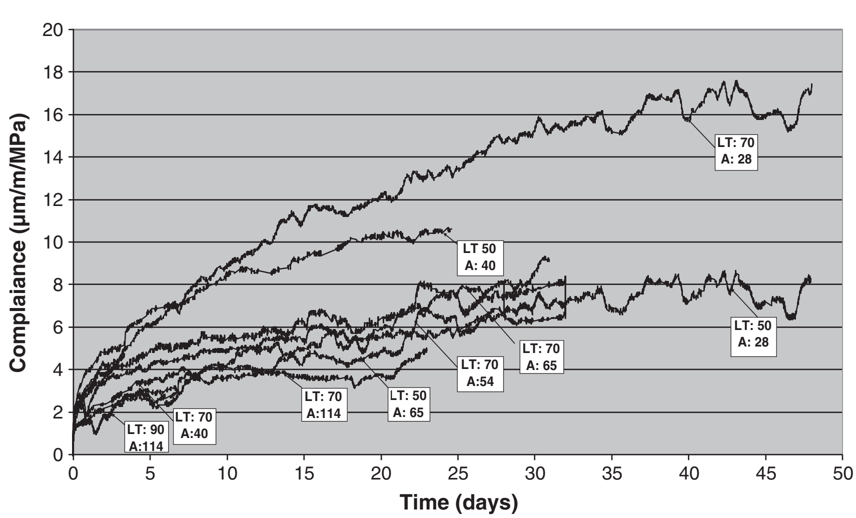

Fig. 19. Compliance curves related to the basic creep in tension for different loading level (L_T) and different concrete ages (A).

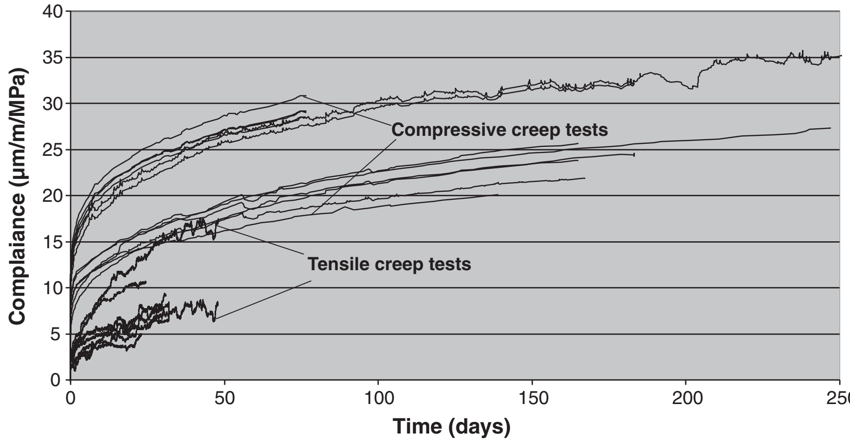

Fig. 20. Summary of the compliance curves related to the basic creep in compression and in tension.

these microcracks. These two types of movement will lead to a drying of the concerned capillaries (reduction in the water meniscuses). This self-drying induced by cracking will cause an additional shrinkage to the well-known one linked to the restrained hydration of the anhydrous cement grains.

From the proposed mechanism, the two following conclusions can be made:

1. The mechanism of drying of the capillaries bordering the cracks depends on two kinetics: one related to Fick's law, and the other one related to Darcy's law.
2. Microcracks, which are formed, cross a large number of hydrates and of anhydrous cement grains. The created microcracks, constituting paths of privileged access for liquid water, will allow a significant acceleration of the kinetics of hydration of anhydrous grains (phenomenon of self-healing of the microcracks), and thus will increase the amplitude and the kinetics of the self-drying shrinkage.

In conclusion, and to summarize the mechanism proposed above, the assumption is made that the basic creep of concrete is mainly due to microcracking which induces additional self-drying shrinkage.

Reinhardt and Rinder [18] proposed also that specimen loaded during a tensile creep test shrank more than unloaded specimens. But in their case, they did not associate the additional shrinkage to the evolution of the concrete cracking.

To evaluate the acceptability of this proposal, it is necessary to answer the two following questions:

- Which physical mechanisms are at the origin of the kinetics of creation of the microcracks during the creep step?
- How to explain that basic creep in tension is much lower than basic creep in compression?

7.1. Physical mechanisms at the origin of the kinetics of microcracking during creep step

The fact that microcracking is at the origin of the basic creep of concrete requires obligatorily that a kinetics of microcracking exists which will generate kinetics of strain during the creep step. The density of microcracks, generated during the creep step, depends on the propagation of the microcracks created during the static loading (initial microcracks), but also on the creation of new microcracks.

7.1.1. Creation of new microcracks

When the capillaries of the concrete are drained in the vicinity of the initial microcracks, induced self-drying shrinkage appears in the surrounding cement paste. The evolution of this self-drying shrinkage will induce an evolution of the stress field in the cement paste. Stresses caused by the presence of grains of sand restraining the shrinkage of this cement paste will change.

Consequently, additional tensile stresses, which did not exist at the end of the static loading, will appear during the creep step. These additional tensile stresses will be able to create new microcracks with kinetics related to the drying of the capillaries.

Table 6
Total specimen volumes and volumes concerned by the displacement measurement.

Specimen type	V_1	V_2	V_3	V_4
Total specimen volume (cm^3)	20096	6633	6431	1520
Volume of material concerned (cm^3)	10048	5306	2412	950

Fig. 21. Experimental setup used for specimen V_1.

Fig. 22. Experimental setup used for specimen V_2.

Fig. 24. Experimental setup used for specimen V_4.

7.1.2. Propagation of the initial microcracks

The analysis of the propagation of the initial microcracks is based on the fracture mechanics of pseudo-fragile materials such as concrete and more precisely on the Barenblatt theory [19].

In the Barenblatt theory, two systems of forces exist at a crack tip.

The first system of force is related to the external loading (here the creep loading). It leads to a tensile stress concentration, concentration whose intensity is described by the stress intensity factor *K*, which depends on the level of the external loading and of the crack length.

Fig. 23. Experimental setup used for specimen V_3.

The second system of forces concerns forces of cohesion (Fig. 26). These forces of cohesion are attractive forces *F* being exerted between the particles on both sides of the plan of separation of the crack (plan AB in Fig. 26) located in a very small zone of width *d*, much smaller than the length *L* of the crack (these are forces of surface). These forces of cohesion depend on spacing *v* of the lips of the crack as indicated in Fig. 27. These forces of cohesion are regarded as a nonlinear function of spacing *v*, and depend obviously on the type of material considered. When *v* reaches a certain value v_m, the forces of cohesion disappear (Fig. 27). This second system of forces also generates a stress concentration at the crack tip, stresses that are opposed to those generated by the external loading. The intensity of this stress concentration is described by the stress intensity factor *k* (which depends on D and v). When the crack does not propagate (is motionless), the factor *k* compensates exactly for the factor *K*. When the crack propagates, that means that the factor *k* does not compensate any more for the factor *K*, and that happens when the crack opening *v* reaches a certain critical value.

In the case of the creep loading, the initial microcrack opening remains theoretically constant since the mechanical loading is constant.

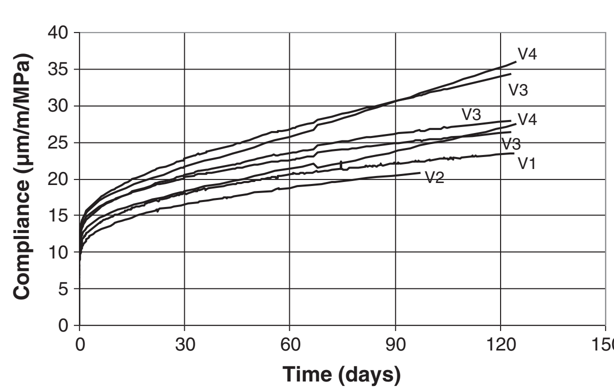

Fig. 25. Compliance curves for all specimens tested (1 V_1, 1 V_2, 3 V_3, and 2 V_4).

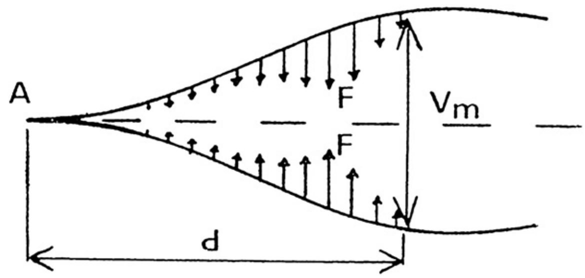

Fig. 26. Forces of cohesion at the crack end.

On the other hand, as has been previously proposed, the creation of the microcracks, during the static loading (initial microcracks), generates liquid water movements towards these microcracks lately created. The presence of this water at the crack end will consequently reduce considerably the forces of cohesion. The stress intensity factor *k* will not be able then to compensate any more for the stress intensity factor *K*, and therefore microcracks will be able to propagate.

In summary, the above explanation is for the creation of new microcracks or the propagation of the initial one, the kinetics of these two phenomena is related to Darcian transport of water from the capillaries towards the microcracks.

7.2. Origin of the difference between basic creeps in compression and tension

This difference can be explained by:

- the density of microcracks before localization which is more important in compression than in tension;
- the difference in orientation of the microcracks compared to the loading direction.

The first explanation is logical and coherent with experiment results presented previously in the paper.

The second explanation requires some elaboration:

- *In compression*, the microcracks are oriented preferentially parallel to the loading direction.
  Consequently, if the assumption that these microcracks induce an additional self-drying shrinkage is considered as valid, this shrinkage can be only anisotropic, i.e. important in the direction parallel to the microcracks and weak in the direction perpendicular to the microcracks.

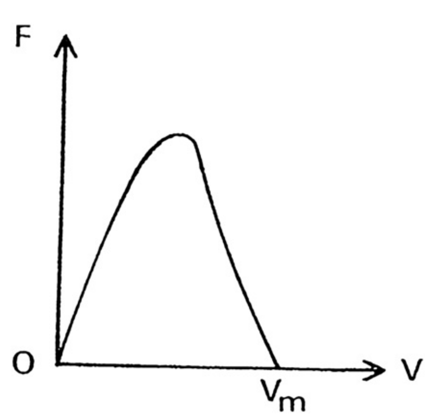

Fig. 27. Shape distribution of the forces of cohesion as a function of the crack opening.

  Therefore, in a creep test in compression, the additional strain induced by the additional self-drying shrinkage is important in the direction of the loading.
  The additional strain of self drying shrinkage should open the existing microcracks and, thus, should increase the apparent Poisson's ratio of the concrete.
- *In tension*, the microcracks are oriented preferentially perpendicular to the loading direction. Consequently, the microcracks will induce an additional self-drying shrinkage, always anisotropic, but important in the direction perpendicular to the loading, and weak in the direction parallel to the loading.

As previously mentioned, the additional strain induced by the additional self-drying shrinkage would have the effect of opening the microcracks. These cracks opening will lead, this time, to a strain opposed to the self-drying shrinkage strain. This strain, induced by the microcracks opening, constitutes the creep strain in tension of concrete.

Fig. 28 presents a schematic illustration of what is described above.

It thus appears obvious that this strain in tension related to the induced opening (by the additional self-drying shrinkage) of the microcracks can be only much lower than the basic creep strain in compression, directly related to the additional self-drying shrinkage.

8. Conclusions

An experimental investigation concerning the use of acoustic emission to analyze the physical mechanisms underlying the basic creep of concrete has been carried out.

The total number of acoustic events recorded and the frequency analysis of the acoustic signals have been made on a basis of 126 days of test.

These results confirm those previously obtained in [2], i.e. that:

- ✔ The basic creep strain is proportional to the total number of microcracks created in the material.
- ✔ The higher the loading level, the higher the density of microcracks created, and the higher the *density of microcracks created/basic creep strain* ratio.

An experimental comparison between the basic creep in compression and the basic creep in tension leads to the following conclusion: *The basic creep of concrete in tension is much lower than the basic creep in compression.*

An experimental study of the volume effects related to the basic creep in compression leads to the following conclusion: *there are no significant volume effects related to creep in compression.*

All these conclusions added to the analysis of the experimental evidences found in literature, permit to propose an assumption concerning the physical mechanisms at the origin of the basic creep of concrete.

This assumption is that the creation of the microcracks during the static loading constitutes the origin of this basic creep. As a matter of fact, these microcracks generate additional strains related to the creation of an additional self-drying shrinkage.

In other words, it is advanced, in this paper, that the basic creep of the concrete is mainly an additional self-drying shrinkage under stress.

Lastly, it is important to state that, to say that the basic creep of concrete is not other than a self-drying shrinkage under stress, inaccurate and useless the summation of strain usually made in the analysis of a creep test. Indeed, one should not any more write this:

$$\varepsilon_{\text{creep}} = \varepsilon_{\text{total}} - \varepsilon_{\text{elastic}} - \varepsilon_{\text{shrrinkage}} - \varepsilon_{\text{thermic}}$$

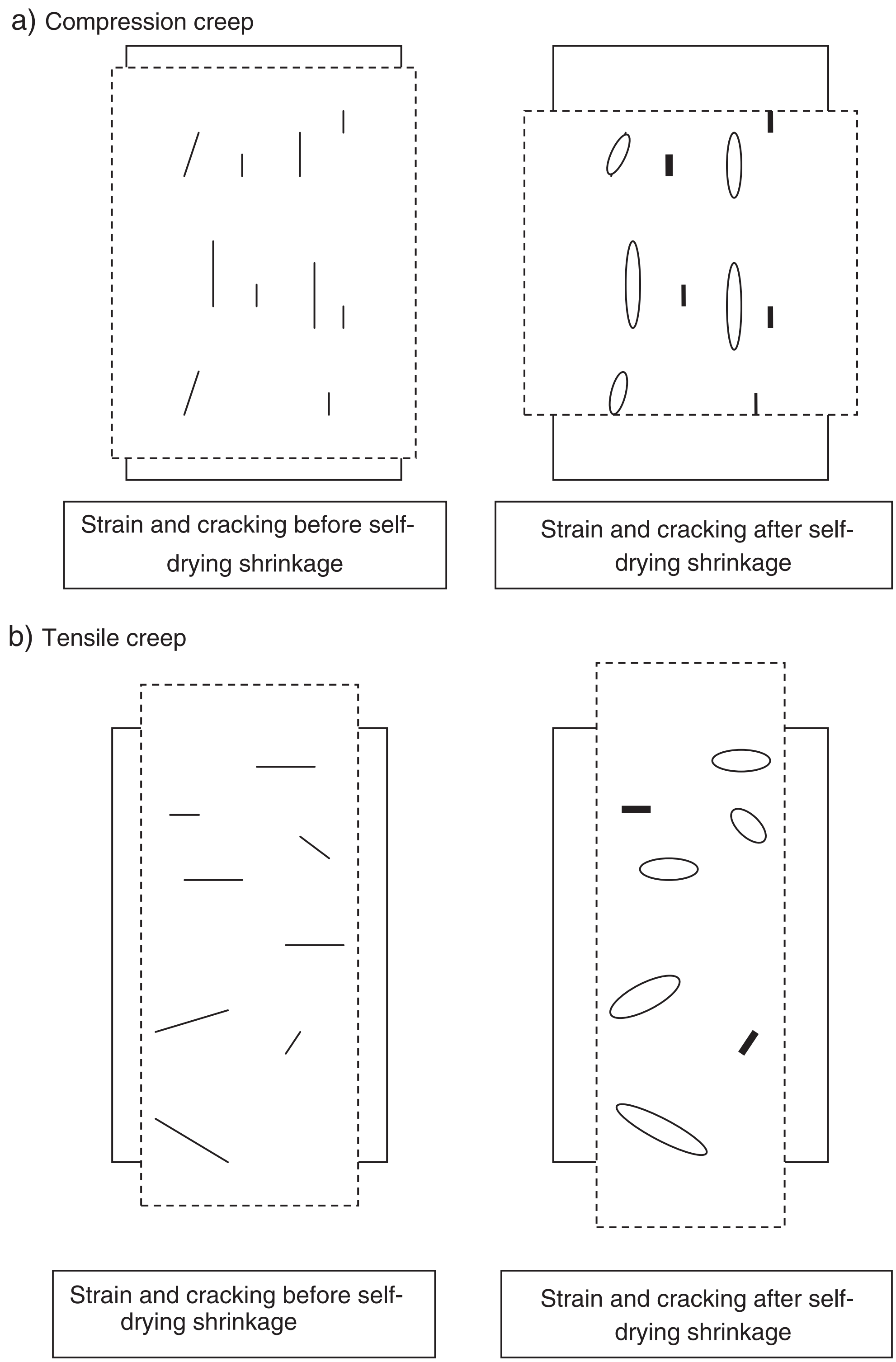

Fig. 28. Process of microcracks opening due to self-drying shrinkage when they are respectively created by compression and tension.

but this:

$\varepsilon_{creep} = \varepsilon_{total} - \varepsilon_{elastic} - \varepsilon_{thermic} = \varepsilon_{ss}$

where ε_{ss} is the shrinkage strain under stress.

Acknowledgments

The authors thank D. Bruhat and R. Michel for their efficient contribution in the use of acoustic emission during this experimental campaign.

References

[1] A.M. Neville, Creep of Concrete: Plain, Reinforced and Prestressed, Noth-Holland Publishing Company, Amsterdam, 1970.
[2] P. Rossi, et al., Investigation of the basic creep of concrete by acoustic emission, Materials and Structures 27 (1994) 510–514.
[3] P. Acker, Measurement of Time Dependent Strains of Concrete Loaded in Compression, Rilem Recommendation, 1993 (June).
[4] F. de Larrard, P. Acker, R. Le Roy, (Chap.3), in: S.P. Shah, S.H. Ahmad (Eds.), Shrinkage, Creep and Thermal Properties, High-Performance Concretes and Applications, Edward Arnold Publ, 1993, pp. 65–114, (Oct).

[5] R. Le Roy, F. de Larrard, Creep and shrinkage of High-Performance concrete : the L.C.P.C. experience, CONCREEP 5, RILEM Symposium, pp. 499–504, Barcelone, September 1993.
[6] L. Granger, J.M. Torrenti, Evaluation of the lifespan of a nuclear PC vessel in terms of delayed behaviour and loss prestress, IABSE Symposium on Extending the Lifespan of Structures, San Francisco, 1995, pp. 1411–1416.
[7] A. Attolou, A. Belloc, J.M. Torrenti, Méthodologie pour une nouvelle protection du béton vis-à-vis de la dessiccation, Bulletin de Liaison des Laboratoires des Ponts et Chaussées, vol. 164, 1989, pp. 85–86, (in french).
[8] P. Rossi, et al., Identification of the physical mechanisms underlying acoustic emission during the cracking of concrete, Materials and Structures 22 (1989) 194–198.
[9] P. Rossi, et al., The use of acoustic emission in fracture mechanics applied to concrete, Engineering Fracture Mechanics 35 (1990) 751–763.
[10] N. Reviron, G. Nahas, J.L. Tailhan, F. Le Maou, F. Benboudjema, A. Millard, Experimental study of uniaxial tensile creep of concrete, Proceedings of the Eighth International Conference on Creep, Shrinkage and Durability of Concrete and Concrete Structures, 2008, pp. 453–457, Ise-Shima, Japan.
[11] J.L. Clément, F. Le Maou, Experimental repeatability of creep and shrinkage concrete tests — data statistical analysis and modelling, Concreep 6, 6th International Conference on Creep, Shrinkage and Durability Mechanics of Concrete and Other Quasi-Brittle Materials, 2001, MIT Cambridge USA.
[12] M. Omar, et al., Creep-damage coupled effects: experimental investigation on bending beams with various sizes, Journal of Materials in Engineering, ASCE 21 (2009) 65.
[13] R.E. Davis, H.E. Davis, E.H. Brown, Plastic flow and volume changes of concrete, Proceedings (ASTM), vol. 37, 1937, pp. 317–330.
[14] J.J. Brooks, A.M. Neville, A comparison of creep, elasticity and strength of concrete in tension and in compression, Magazine of Concrete Research 29 (11) (1977) 131–141.
[15] P. Rossi, et al., Scale effect on concrete in tension, Materials and Structures 27 (1994) 437–444.
[16] G. Carpinteri, G. Ferro, Ventura, Scale-independent constitutive law for concrete in compression, Convegno IGF 17, 2004.
[17] W. Weibull, A statistical theory of the strength of material, Ing. Vet. ak. Han, 1939, n°51.
[18] H.W. Reinhardt, T. Rinder, Tensile creep of high-strength concrete, Journal of Advanced Cement Technology 4 (2008) 453–457.
[19] G.I. Barenblatt, Advanced Applied Mechanics 7 (1962) 55.